Materials Chemistry and Physics 138 (2013) 286–294

Contents lists available at SciVerse ScienceDirect

Materials Chemistry and Physics

journal homepage: www.elsevier.com/locate/matchemphys

Polymer/surfactant assisted self-assembly of nanoparticles into Langmuir–Blodgett films

T. Alejo [a], M.D. Merchán [a], M.M. Velázquez [a,*], J.A. Pérez-Hernández [b]

[a] Departamento de Química Física, Facultad de Ciencias Químicas, Universidad de Salamanca, Plaza de los Caídos s/n, E-37008 Salamanca, Spain
[b] Centro de Láseres Pulsados Ultraintensos (CLPU), E-37008 Salamanca, Spain

HIGHLIGHTS

- Effect of the composition on the LB films of QDs/polymer.
- Effect of the composition on the LB films of QDs/Gemini surfactant.
- Dewetting mechanisms.

GRAPHICAL ABSTRACT

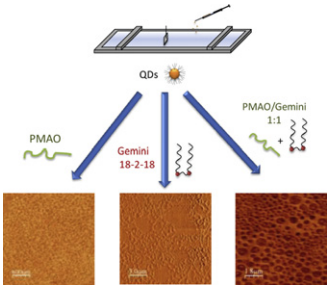

ARTICLE INFO

Article history:
Received 1 August 2012
Received in revised form
5 November 2012
Accepted 18 November 2012

Keywords:
Polymers
Nanostructures
Thin films
Atomic force microscopy (AFM)
Electron microscopy (SEM)

ABSTRACT

We studied the ability of poly(octadecene-co-maleic anhydride) (PMAO) and a Gemini surfactant [$C_{18}H_{37}(CH_3)_2N^+Br^-–(CH_2)_2–N^+Br^-(CH_3)_2\ C_{18}H_{37}$] (18-2-18) to assist in the self-assembly process of CdSe quantum dots (QDs) at the air–water interface. Results show that, while QD agglomeration is generally inhibited by the addition of these components to the Langmuir monolayer of QDs, structure of the film transferred onto mica by the Langmuir–Blodgett method is strongly affected by the dewetting process. Nucleation-and-growth of holes and spinodal-like dewetting were respectively observed in the presence of either PMAO or 18-2-18. When PMAO/18-2-18 mixtures were used, both mechanisms were allowed; nevertheless, even in films prepared with mixtures of low polymer contents, characteristic morphology from the polymer dewetting route prevailed.

1. Introduction

Self assembly is established as a very interesting technique in the preparation of many different types of nanomaterials. Specifically, thin films of soft matter can provide templates for the fabrication of devices based on QDs in an attempt to achieve sufficiently dispersed nanomaterials in which the agglomeration of nanoparticles was minimized [1].

Many techniques and materials have been used in the preparation of QDs with a focus on the optimization of self-assembled monolayers. A common strategy employs a template to control the deposition during solvent evaporation. However, template fabrication usually involves lithography processes, and this method is often limited because special equipment is required. In this paper, we focus on the Langmuir Blodgett methodology (LB) to obtain self-assemblies of CdSe QDs. We chose this technique because it has proved to be a versatile and interesting method to obtain thin films with a molecular density that can be readily modified by compressing or expanding the film using a barrier. The LB methodology allows continuous variation of the particle density, spacing, and

* Corresponding author. Fax: +34 923294500x1547.
E-mail address: mvsal@usal.es (M.M. Velázquez).

0254-0584/$ – see front matter © 2012 Elsevier B.V. All rights reserved.
http://dx.doi.org/10.1016/j.matchemphys.2012.11.058

even arrangement. Some dewetting processes have been observed in the preparation of the LB films; however, they can be used to achieve different patterns without a defined template [1–3].

Various attempts to immobilize QDs onto solids substrates by the LB technique have been reported offering the possibility of fabricating a wide range of organic/inorganic LB films [3]. The main efforts are focused on the preparation of fine dispersions of nanoparticles inside polymers so that the photophysical properties of the nanocrystals are not affected [4]. However, the poor compatibility of the QDs with the polymers leads to agglomeration of the nanoparticles inside the films even at low concentrations, these agglomerates result in a loss of the nanoparticle optical properties. Some theoretical arguments have suggested that the interactions between self-organizing particles and a self assembling matrix material can produce ordered structures [5]. Thus, diblock copolymers are known to self-assemble spontaneously into structures on the order of tens of nanometers in length, and these structures can be transferred onto substrates by LB or dip-coating methods [6–8]. Specifically, some research revealed that the organization of nanoparticles is governed by molecular interactions between the diblock copolymers and nanoparticles that constitute the mixed monolayers at the air/water interface [9,10]. Despite some successful results, more efforts must be carried out to develop nanometric structures that may provide new properties associated with the reduction of the materials size [11,12]. With this objective in mind, we focus attention on the self-assembly process of CdSe nanocrystals onto solid substrates assisted by the copolymer poly (octadecene-co-maleic anhydride) (PMAO). We chose this polymer because it has demonstrated to be a good stabilizer of CdS nanoparticles in form of reversed micelles [13]. Moreover, the PMAO-capped CdS nanoparticles have been efficiently transferred from the air–water interface onto solids. On the other hand, the polymer PMAO showed high compatibility with magnetic nanoparticles [14] and thin films of PMAO were used with QDs for the preparation of biosensors [15].

Another way to improve the compatibility of QDs coated by trioctylphosphine oxide (TOPO) with the air–water interface or with the solid substrates is to replace TOPO by surfactant molecules such as 1-octadecanethiol (ODT) or oleic acid [16], or amphiphilic compounds such as mercaptosuccinic acid (MSA) [17] and sodium hexametaphosphate, which increases the adsorption of the nanoparticles on the interfaces [18]. Gemini surfactants made of two surfactant monomers linked by a spacer chain display excellent amphiphilic properties such as high adsorption capacity on solid surfaces, which make them excellent candidates to stabilize nanoparticles in aqueous medium [19,20], to assist in the self-assembly process [21–24] and in the growth of nanoparticles with a defined geometry [25]. Accordingly, we are interested in exploring the effect of a Gemini surfactant on the self-assembly process of QDs adsorbed on mica. Therefore we chose the cationic Gemini surfactant ethyl-bis (dimethyl octadecylammonium bromide), referred to as 18-2-18 hereafter, to prepare mixed Langmuir monolayers with QDs and to transfer these monolayers onto mica by the LB methodology. In a previous work we showed that the LB films of 18-2-18 are constituted by surfactant molecules adsorbed on the solid interface leading to a uniform and continuous film indicating that the surfactant spreads well [26] and consequently, we hope that the surfactant improves the QDs adhesion on the solid substrate.

Finally, it is well established that mixtures containing polymer and surfactant molecules provide synergistic effects in the aggregation process of these molecules in solution [27] and in the surface properties of the monolayers [28–33]. We expect to find synergistic effects on the self-assembly of QDs at the interface by means of mixtures of the polymer PMAO and the Gemini surfactant 18-2-18. Therefore, looking towards synergy in the molecular interactions between PMAO/Gemini and QDs, we analyze the structure of films obtained by transferring Langmuir monolayers composed by PMAO, 18-2-18 and CdSe QDs from the air–water interface onto solids by the LB methodology. Taking into account that small changes on the surface composition lead to structures with different architectures, we address the study to evaluate the effect of the surface composition on the self-assembly process at the interface to prepare LB films with different morphologies. According to the objectives proposed, the work is organized in two parts. First, we deal with the study of two-component Langmuir systems containing PMAO or 18-2-18 Gemini surfactant and CdSe QDs, and second, the properties of films composed by mixtures of the three components are analyzed. Because the preparation of LB films requires the knowledge of the Langmuir monolayers precursors of these films, we previously studied the properties of Langmuir monolayers by recording the surface pressure and elasticity isotherms. Finally, we evaluate the morphology of the LB films by AFM, SEM and ellipsometry.

2. Materials and methods

2.1. Materials

Gemini surfactant ethyl-bis (dimethyl octadecylammonium bromide), 18-2-18, (Mr = 783.02) was synthesized using the method described by Zana et al. [34] with some modifications in the purification procedure we introduced to improve the purity of the product [26]. The product was characterized by mass spectrometry and nuclear magnetic resonance to guarantee a degree of purity >99.9%, necessary for the correct interpretation of surface experiments. Polymer poly (maleic anhydride-alt-1-octadecen), PMAO (Mr = 40 kDa) was purchased from Sigma–Aldrich and was used without purification.

The hydrophobic CdSe QDs were synthesized by the method proposed by Yu and Peng [35]. This method uses cadmium oxide and Se powders as precursors. First, cadmium oxide, oleic acid and octadecene were loaded into a flask with a condenser assembly under Ar flow and agitation. The mixture was heated to 210 °C obtaining a clear and colorless solution and then the solution of trioctylphosphine selenide was injected. Nucleation and growth of the CdSe QDs occurred until the desired particle size was reached by controlling both the temperature and the reaction time. QDs were collected as powder by size-selective precipitation with acetone and dried under vacuum. The QD size (3.4 ± 0.1 nm) was determined by the position of the maximum of the visible spectrum of the QDs dispersed in chloroform [36]. The concentration of nanocrystals was calculated from the UV–vis absorption spectrum of QDs dissolved in chloroform by using the extinction coefficient per mole of nanocrystals at the first excitonic absorption peak [36]. UV–vis absorption spectra of QDs dissolved in chloroform were recorded on a Shimadzu UV-2401PC spectrometer.

Chloroform (PAI, filtered) used to prepare the spreading solutions was from Sigma–Aldrich. Millipore ultra pure water prepared using a combination of RiOs and Milli-Q systems from Millipore was used as subphase. The LB substrate muscovite (mica) quality V-1 was supplied by EMS (USA). The mica surface was freshly cleaved before use. The solid substrate Si (100) wafers were used without pretreatment to obtain the ellipsometric measurements and were supplied by Siltronix (France).

2.2. Preparation of Langmuir monolayers and Langmuir–Blodgett films

The surface pressure measurements were performed on two computer-controlled Teflon Langmuir film balances, Minitrough

and Standard KSV2000-2 (KSV, Finland). Spreading solution (1×10^{-4} M) was deposited onto water subphase using a Hamilton microsyringe. The syringe precision is 1 μL. The surface pressure was measured with a Pt-Wilhelmy plate connected to an electrobalance. The subphase temperature was maintained at (20.0 ± 0.1) °C by flowing thermostated water through jackets at the bottom of the trough. The water temperature was controlled by means of thermostat/cryostat Lauda Ecoline RE-106. The temperature near the surface was measured with a calibrated sensor from KSV. Langmuir monolayers were transferred by symmetric barrier compression (5 mm min^{-1}) with the substrate in the trough by vertically dipping it up at a rate of 5 mm min^{-1}.

The film composition at the air–water interface is expressed as follows: when the film is composed of two components, the polymer or surfactant matrix and the QDs nanoparticles, the composition is expressed as mole fraction of PMAO or Gemini at the surface, X_{PMAO} or X_{Gemini}, respectively: $X_{PMAO\ or\ Gemini} = n_{PMAO\ or\ Gemini}/(n_{PMAO\ or\ Gemini} + n_{QD})$. In contrast, when the matrix is composed of a binary mixture of PMAO and surfactant, all the experiments were carried out by keeping constant the matrix mole fraction, X_{Matrix}, $X_{Matrix} = n_{PMAO}+n_{Gemini}/(n_{PMAO} + n_{Gemini} + n_{QD})$ at 0.98 and modifying the matrix composition. Accordingly, the matrix composition was expressed in terms of PMAO mole fraction, Y_{PMAO}, $Y_{PMAO} = n_{PMAO}/(n_{PMAO} + n_{Gemini})$. In these equations n_{Gemini} and n_{QD} are the amount of Gemini surfactant and QDs, respectively, and n_{PMAO} represents the amount of polymer in terms of repeat unit.

2.3. Scanning electron microscopy (SEM)

A FEI Helios 450 dual-beam FIB/SEM was used to obtain images of the LB films with a supply to the electron beam between 5 and 10 kV.

2.4. Atomic force microscopy (AFM)

AFM images of the LB films on mica substrates were obtained in constant repulsive force mode by AFM (Nanotec Dulcinea, Spain) with a rectangular microfabricated silicon nitride cantilever (Olympus OMCL-RC800PSA) with a height of 100 μm, a Si pyramidal tip and a spring constant of 0.73 N m^{-1}. The scanning frequencies were usually in the range between 0.5 and 2.0 Hz per line. The measurements were carried out under ambient laboratory conditions.

2.5. Ellipsometry

Ellipsometric measurements were performed on a null imaging ellipsometer (Nanofilm, model EP3, Germany) to determine the refractive index and the thickness of the Langmuir–Blodgett films. The incident Nd:YAG laser beam ($\lambda = 532$ nm) was focused on the LB films on silicon substrates positioned on the goniometer plate at a fixed incident angle of 70°. Each sample was measured in several regions to obtain representative values. The precision on the ellipsometric angles is ca. 0.0006. The interface was modeled with the three layers model previously described [37]. The first one is the Si substrate with a refractive index of 4.1264 and the second layer is a native oxide layer with a refractive index of 1.4653 [38,39], which were obtained in an ellipsometry experiment using a clean Si wafer. The thickness and refractive index of the QDs films on different matrix were obtained by fitting the ellipsometric angles, Δ and Ψ, to Fresnel equation.

3. Results and discussion

3.1. Mixed monolayers and Langmuir–Blodgett films of PMAO and CdSe QDS

With the purpose of organizing QDs into ordered two-dimensional (2D) arrays, we transferred mixed monolayers of polymer PMAO and CdSe QDs from the air–water interface onto mica by the Langmuir–Blodgett (LB) methodology. We prepared films containing different surface composition, expressed in polymer mole fraction units, X_{PMAO}, to evaluate the effect of the templates on the self-assembly process.

It is well established that the properties of mixed monolayers depend on the spreading technique [31,40]. For two-component mixtures, the methods used for Langmuir monolayers preparation consist of spreading a solution containing both components, named co-spreading, and the spreading of the components separately. We tested these methodologies and found that in all cases the isotherms are very stable, and the densest and most reproducible monolayers were obtained by the co-spreading method. As this behavior was observed for all the mixtures, this method was chosen to prepare the mixed Langmuir monolayers precursors of the LB films. This method proved to be the best one to obtain stable mixed monolayers of surfactant/polymers [31], polymer/nanoparticles [41] and surfactants [40].

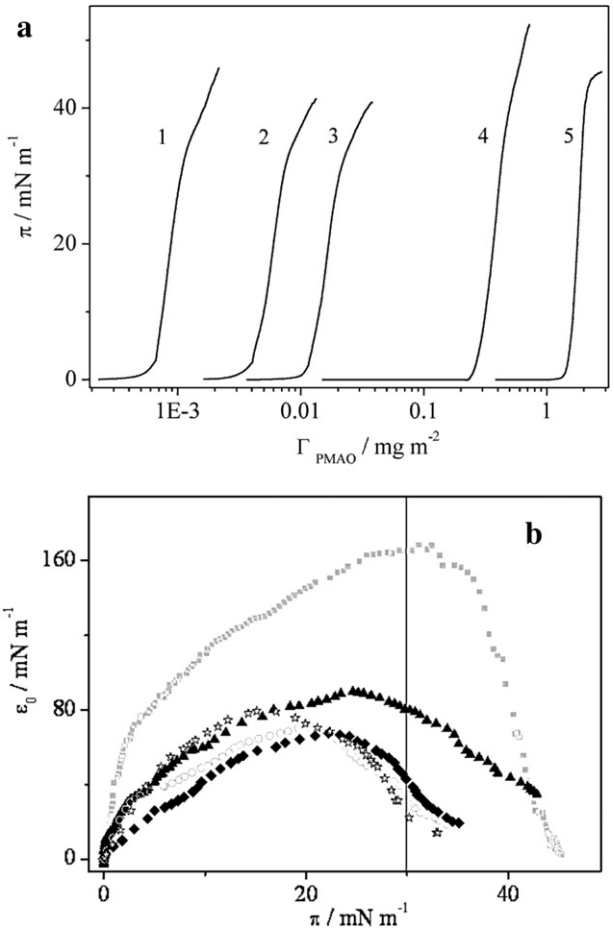

Fig. 1. (a) Surface pressure isotherms of PMAO/QDs mixed Langmuir monolayers at polymer mole fraction of: 0.1 (1); 0.5 (2); 0.75 (3); 0.98 (4); pure PMAO (5). (b) Equilibrium surface elasticity modulus vs. surface pressure of PMAO/QDs mixed Langmuir monolayers at polymer mole fraction of: 0.1 (stars); 0.5 (rhombi); 0.75 (open circles); 0.98 (triangles); pure PMAO (closed circles).

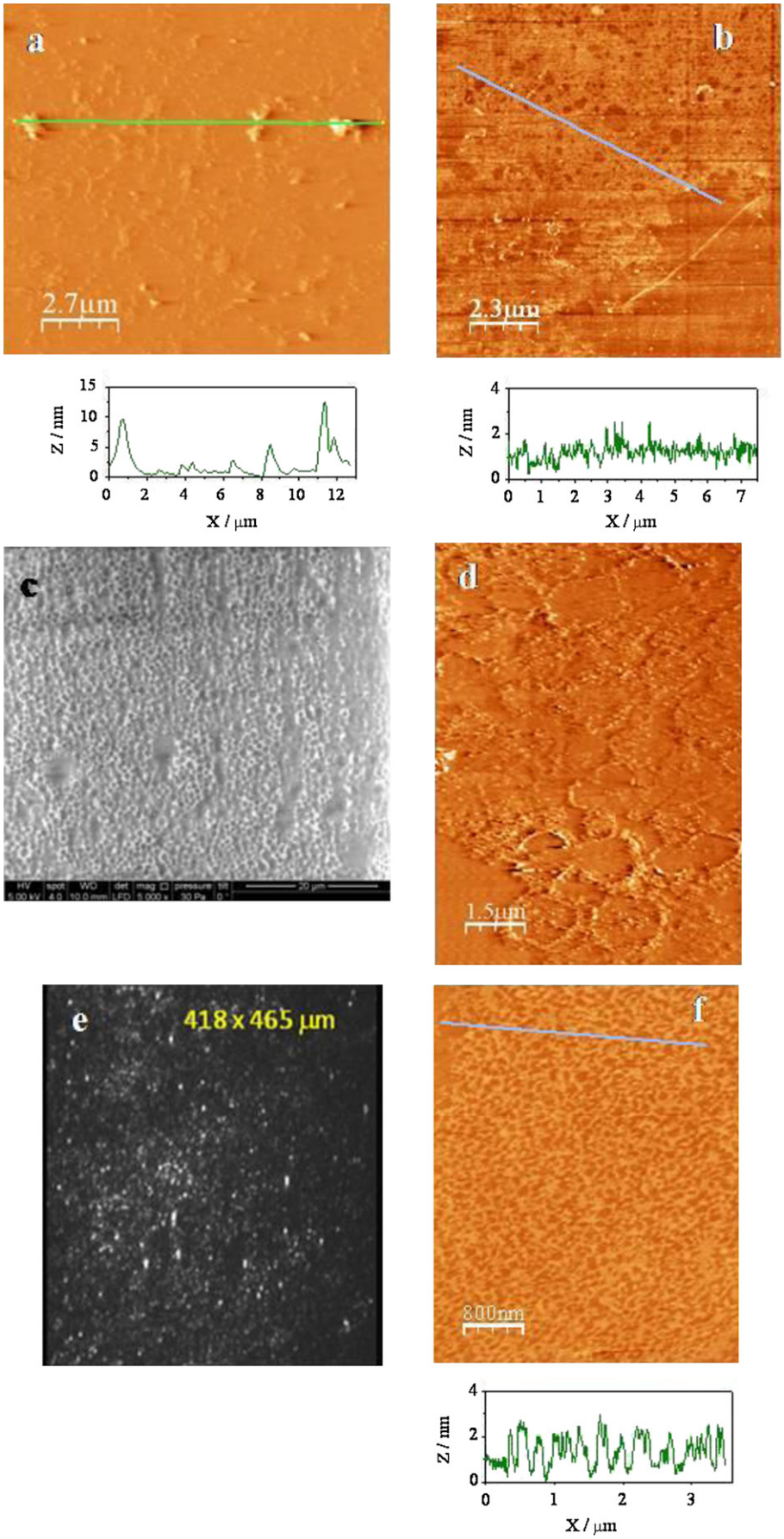

Fig. 2. (a) AFM image of QDs transferred onto mica. (b) AFM image of PMAO transferred onto mica. SEM (c) and AFM (d) images of PMAO/QDs LB film at polymer mole fraction of 0.50. Images obtained by ellipsometry (e) and AFM (f) of PMAO/QDs LB films at polymer mole fractions of 0.98. The Langmuir monolayers were transferred at the surface pressure of 30 mN m^{-1}.

Fig. 1a presents the isotherms of PMAO and PMAO/QDs mixed monolayers. As can be seen in Fig. 1a, the morphology of these curves changes with the surface composition. To gain insight into the states of the monolayers, we calculated the equilibrium elasticity modulus from the surface pressure isotherms and the equation: $\varepsilon_0 = \Gamma(\delta\pi/\delta\Gamma)_T$ [42]. Results are represented in Fig. 1b as a plot of ε_0 against the surface pressure values. The surface pressure and elasticity isotherms for the polymer PMAO presents a trend characteristic of polymeric monolayers in which the elasticity modulus increases with the surface concentration until it reaches a maximum value. Beyond the maximum, ε_0 decreases because the polymer molecules are too close and the conformational degrees of freedom of the polymer chains decrease, and as a consequence, the elasticity also decreases [31,38]. Before the maximum, ε_0 rises with a different rate below and above a given surface pressure value of 4 mN m^{-1}; at this surface pressure the ε_0 value is around 98 mN m^{-1} and corresponds to the onset of the liquid condensed (LC) state.

In PMAO/QDs mixed monolayers, ε_0 drastically decreases compared with the values of the polymer monolayer. This behavior is observed even in monolayers with small concentrations of QDs, $X_{QD} = 0.02$. In contrast to PMAO monolayer, the elasticity values for the mixed PMAO/QDs monolayers correspond to liquid expanded states (LE). This behavior points to an interdigitation of the polymer chains with the QDs stabilizer (TOPO). Thus, the interdigitation of PMAO and QDs avoids the interaction between the polymer molecules avoiding the formation of the polymer LC state.

Langmuir films were transferred at a surface pressure of 30 mN m^{-1} from the air–water interface onto solid substrates by the LB methodology. We use this surface pressure because we want to obtain high coverage in the QDs LB films. Moreover, 30 mN m^{-1} matches with the maximum elasticity of the polymer monolayer where one expects to achieve the maximum arrangement of the nanoparticles on the polymeric matrix. The morphology of the LB films was analyzed by ellipsometry, SEM and AFM.

Fig. 2 presents the images obtained using different techniques of several mixed PMAO/QDs LB films. For the sake of comparison the AFM image and the roughness obtained from AFM of the LB film of the two separate components, QDs and PMAO, at 30 mN m^{-1} are collected in Fig. 2a and b, respectively. As can be seen in Fig. 2a, QDs form agglomerates with different roughness. This behavior was referred previously [10] and it was related to the weak interactions between the hydrophobic chains of the QDs stabilizer (TOPO) and the solid substrate, mica. The LB film of PMAO presents some holes produced by dewetting process. The growth of holes appears when the gravity contribution dominates over the interfacial energy and the van der Waals forces. In this situation, the film breaks and the material is displaced to the rims of holes [43].

Results in Fig. 2 show that the addition of the polymer PMAO increases the surface coverage of QDs. This fact can be interpreted if one considers that the QDs can be adsorbed on the polymer by attractive interactions between the polymer chains and the QDs stabilizer, TOPO, improving QDs adhesion on the solid wafer. The images in Fig. 2 support the idea of an evolution in the morphology of the QDs films as a function of the PMAO surface composition. Fig. 2c presents the SEM image of the monolayer at $X_{PMAO} = 0.50$. The figure shows an apparently well-organized hexagonal mosaic, which when observed at a smaller scale (see Fig. 2d), shows the coexistence of different kinds of aggregates, open hexagonal structures and agglomerates. The hole size of the hexagonal domains was measured from the SEM and AFM images by taking an average of 25 holes per sample and the statistical results are presented in Table 1. The roughness determined from AFM profiles depends on the aggregates chosen. It is interesting to note that the roughness of rims around the holes was 3 nm and it is compatible with the diameter of the CdSe QDs dissolved in chloroform (3.4 nm). The thickness value obtained by ellipsometry was (5.0 ± 0.3) nm and it is slightly higher than the roughness determined by AFM. This can be interpreted if one considers that ellipsometry analyzes a much larger region than AFM, and the thickness value determined by ellipsometry is the average of the thicknesses of different aggregates in the selected

Table 1
Average hole and rim size values of hexagonal domains observed in LB films.

Matrix	X_{Matrix}	Hole size[a]		
		X-direction/μm	*Y*-direction/μm	Rim size/μm
PMAO	0.50	2.1 ± 0.5	1.7 ± 0.7	
	0.75	1.2 ± 0.21	1.1 ± 0.4	
	0.98	0.16 ± 0.09	0.14 ± 0.06	0.10 ± 0.02
PMAO/Gemini $Y_{PMAO} = 0.1$	0.98	1.1 ± 0.7	1.0 ± 0.6	0.17 ± 0.06
PMAO/Gemini $Y_{PMAO} = 0.5$	0.98	0.6 ± 0.3	0.4 ± 0.1	0.33 ± 0.08
PMAO/Gemini $Y_{PMAO} = 0.67$	0.98	0.5 ± 0.3	0.5 ± 0.3	0.15 ± 0.05
PMAO/Gemini $Y_{PMAO} = 0.8$	0.98	0.8 ± 0.5	0.6 ± 0.3	0.17 ± 0.05

[a] Reported values are averages and error represents the standard deviation determined from at least 25 surface features

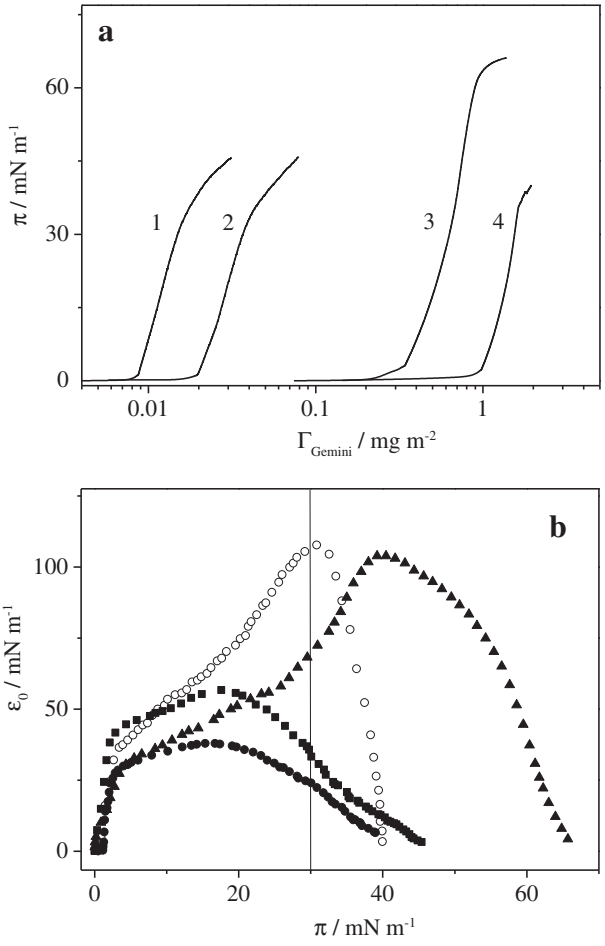

Fig. 3. (a) Surface pressure isotherms of Gemini/QDs mixed Langmuir monolayers at surfactant mole fraction of: 0.5 (1); 0.75 (2); 0.98 (3); pure Gemini (4). (b) Equilibrium surface elasticity modulus vs. surface pressure of Gemini/QDs mixed Langmuir monolayers at surfactant mole fraction of: 0.5 (squares); 0.75 (closed circles); 0.98 (triangles); pure Gemini (open circles).

region. When the polymer concentration is further increased until $X_{PMAO} = 0.98$, a continuous film of QDs is observed. An illustrative example of this fact is the image obtained by the ellipsometer presented in Fig. 2e. The AFM image, Fig. 2f, allows us to observe in detail the film structure. The image in Fig. 2f shows the material accumulation in the rims delimiting a hexagonal network. The diameter of the holes was 0.16 μm and the rim roughness value was ~3 nm, compatible with the QDs diameter in solution. The formation of mosaics has been studied both theoretically and experimentally and was attributed to the dewetting processes; in this system the morphology of the mosaic points to the mechanism referred to as nucleation and coalescence of holes [43]. In this mechanism, the gravity contribution dominates and the process starts with the nucleation of holes at defect sites of the film and the subsequent displacement of material away from the nucleus. The material is accumulated in the rims of holes delimiting a mosaic [44–46]. A theoretical model based on the cell dynamic method proposed the formation of hexagonal networks in films of block copolymers and nanoparticles when the nanoparticle concentration was ~3.2% [47,48]. Our results are consistent with this model because a continuous and uniform film composed by hexagonal features are observed at $X_{QD} = 0.02$. Our work extends the surface composition range as compared with previous work [47,48], demonstrating that when the QDs mole fraction increases above 0.25, the polydispersity of the holes in the network increases and at $X_{QD} \geq 0.50$, the hexagonal network coexists with agglomerates of QDs. These agglomerates predominate when the QDs concentration increases above 0.9, $X_{QD} \geq 0.9$. This behavior indicates that at a given QDs concentration, the attractive interactions between the QDs start to drive the adsorption on the solid substrates leading to the QDs agglomeration.

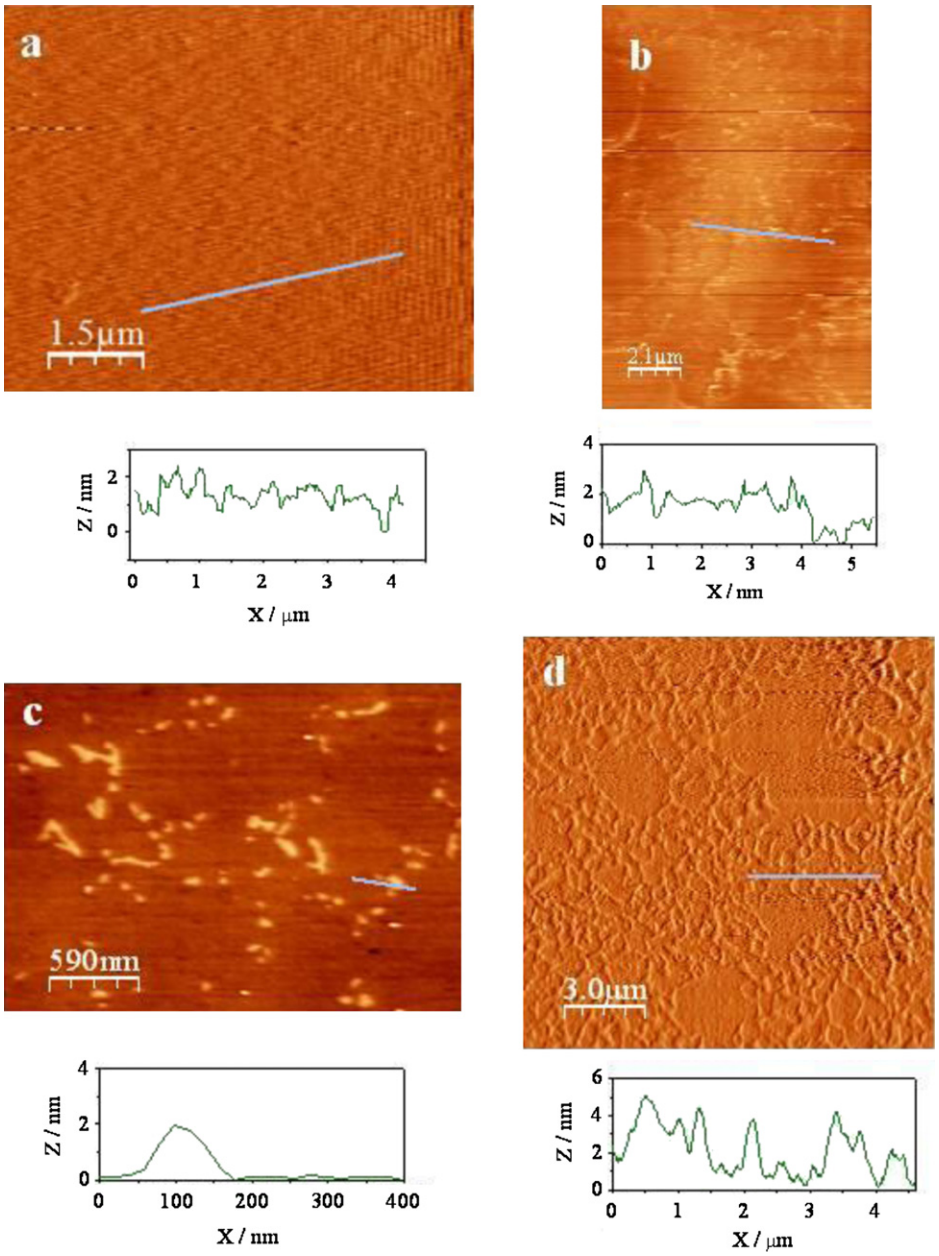

Fig. 4. (a) AFM image of Gemini surfactant transferred onto mica. Images obtained by AFM of Gemini/QDs LB films at surfactant mole fraction of: (b) 0.50; (c) 0.75 and (d) 0.98. The Langmuir monolayers were transferred at a surface pressure of 30 mN m^{-1}.

3.2. Mixed films of the Gemini surfactant 18-2-18 and QDs

An alternative methodology to modulate the QDs self-assembly consists in coating them with surfactant molecules [18–21,24–26]. We want to explore this alternative transferring mixed Langmuir monolayers of the cationic Gemini surfactant 18-2-18 and QDs from the air–water interface onto mica substrate. We chose this surfactant because it has the same hydrocarbon chain length (C_{18}) as the polymer PMAO but a different hydrophilic head group that could drive the self-assembly process in a different way. On the other hand, the surfactant 18-2-18 forms homogeneous LB films on mica indicating important interactions with the solid substrate [26]. This fact can improve the adhesion of QDs on the substrate.

Previously to the LB deposition the surface pressure isotherms of different mixtures were recorded, as shown in Fig. 3a. For comparative purposes the isotherms are represented in terms of surfactant concentration expressed as mg m^{-2} to maintain the same units as in the polymer isotherms. Fig. 3b presents the elasticity isotherms against the surface pressure values. As can be seen in Fig. 3a, the most compressed monolayer corresponds to the pure surfactant. The saturation pressure reaches the highest values for the isotherms with low QDs concentration ($X_{Gemini} \geq 0.98$).

The elasticity value of the surfactant monolayer increases as the surfactant concentration increases and it reaches a maximum value at 30 mN m^{-1}, as shown in Fig. 3b. Beyond the maximum, the elasticity decreases due to the decrease of the conformational degrees of freedom of the surfactant molecules [31,38]. The addition of QDs to the monolayer decreases the elasticity of the surfactant monolayer. This behavior is compatible with the decrease of the conformational degrees of freedom of the surfactant molecules, probably due to the QDs adsorbed on the surfactant chains.

The surfactant/QDs films were transferred from the air–water interface onto mica by the LB method. For the sake of comparison, the surface pressure of the Langmuir monolayer transferred was 30 mN m^{-1}. Images obtained by ellipsometry, SEM and AFM of representative LB films are collected in Fig. 4. The AFM image of the surfactant LB film is presented in Fig. 4a and shows a continuous film of surfactant molecules of roughness ~2 nm. This value is close to the length of the fully extended chain of the surfactant molecule 2.4 nm [27].

Fig. 4b–d show that the surfactant 18-2-18 also increases the surface coverage of QDs and the explanation is quite similar to that proposed to interpret this behavior in PMAO/QDs films, i.e. the QDs stabilizer (TOPO) interacts with the surfactant chains and the head group of the surfactant favors its adsorption on the solid. The AFM images in Fig. 4b–d, show that in mixed surfactant/QDs films, the QDs aggregate in domains of different shapes and that the density of domains increases as the surfactant concentration in the monolayer increases. Comparison between the self-assemblies of PMAO/QDs and surfactant/QDs films shows that the morphologies are quite different pointing to a different dewetting mechanism. Thus, the PMAO/QDs films are constituted by hexagonal networks, while the surfactant/QDs mixed films present some arrays of droplets. The morphology of the surfactant/QDs mixed films was previously observed for films in which the gravitational energy is negligible compared with the capillary effects. In this mechanism, referred as spinodal dewetting, the capillary waves break the film into nanostructures when the amplitude of the capillary waves exceeds the thickness of the film [49]. Differences observed in the dewetting mechanism of PMAO/QDS and surfactant/QDs films can be related with the different molecular weights of the matrix. Thus the molecular weight of the polymer, 40 kD, is higher than the one of the surfactant molecule (Mr = 783.02); accordingly, one expects that the gravitational effects dominate in films containing the polymer because it has a higher molecular weight than the surfactant 18-2-18.

3.3. Three-component, PMAO/Gemini surfactant/QDs, mixed films

It is well established that polymer/surfactant mixtures present important synergistic effects on the surface properties [28–33] and on the self-assembly processes [27]. In the case of the surfactant and the polymer molecules used in this work, previous work demonstrated that PMAO-surfactant (DODAB) [31] and Gemini 18-3-18 and stearic acid mixtures improve the properties of the pure component monolayers, giving a synergistic effect and highly packed monolayers [50]. Therefore we are interested in assessing the synergistic effect of the polymer PMAO and surfactant 18-2-18 mixtures into the self-assembly process of QDs. With this objective in mind, we studied the effect of polymer/surfactant matrix composition on the morphology of QDs LB films.

We worked with films prepared using a matrix composed of binary mixtures of PMAO and surfactant at different compositions, expressed as polymer mole fraction Y_{PMAO}. All the experiments were carried out by keeping X_{Matrix} constant at 0.98. We choose this Matrix/QDs composition because this is the ratio that renders the

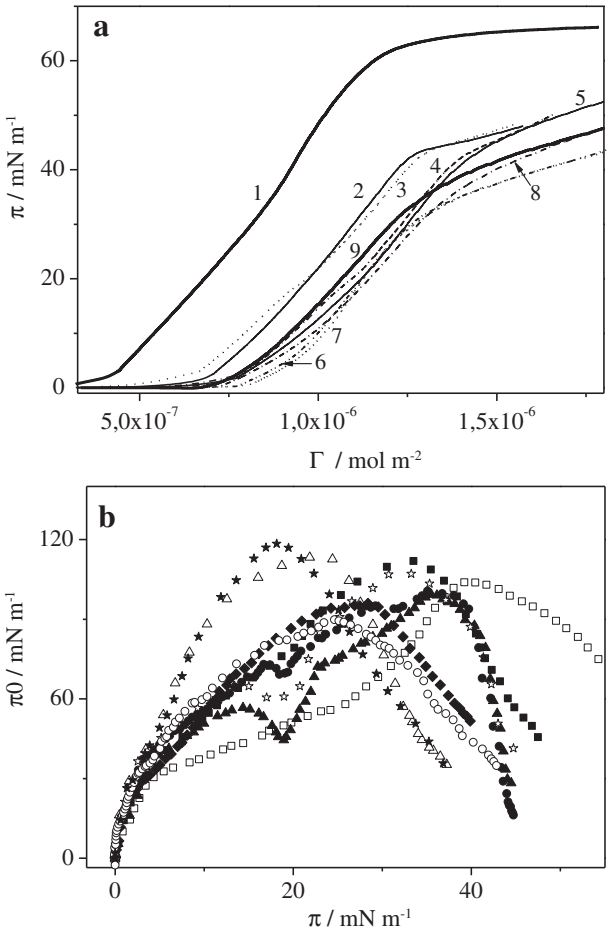

Fig. 5. (a) Surface pressure isotherms of PMAO/Gemini/QDs three-component mixed monolayers prepared by keeping X_{Matrix} constant at 0.98 and the following matrix composition Y_{PMAO}: 0.1 (2); 0.2 (3); 0.33 (4); 0.5 (5); 0.60 (6); 0.67 (7) and 0.8 (8). Lines 1 and 9 represent the isotherms of Gemini/QDs (1) and PMAO/QDs (9). (b) Equilibrium surface elasticity modulus vs. surface pressure values calculated from the isotherms of Fig. 5a for different matrix compositions, Y_{PMAO}: 0.1 (closed circles); 0.2 (triangles); 0.33 (open stars); 0.5 (closed squares); 0.6 (open triangles); 0.67 (closed stars) and 0.8 (rhombi). The values represented by open squares and open circles correspond to Gemini/QDs and PMAO/QDs monolayers.

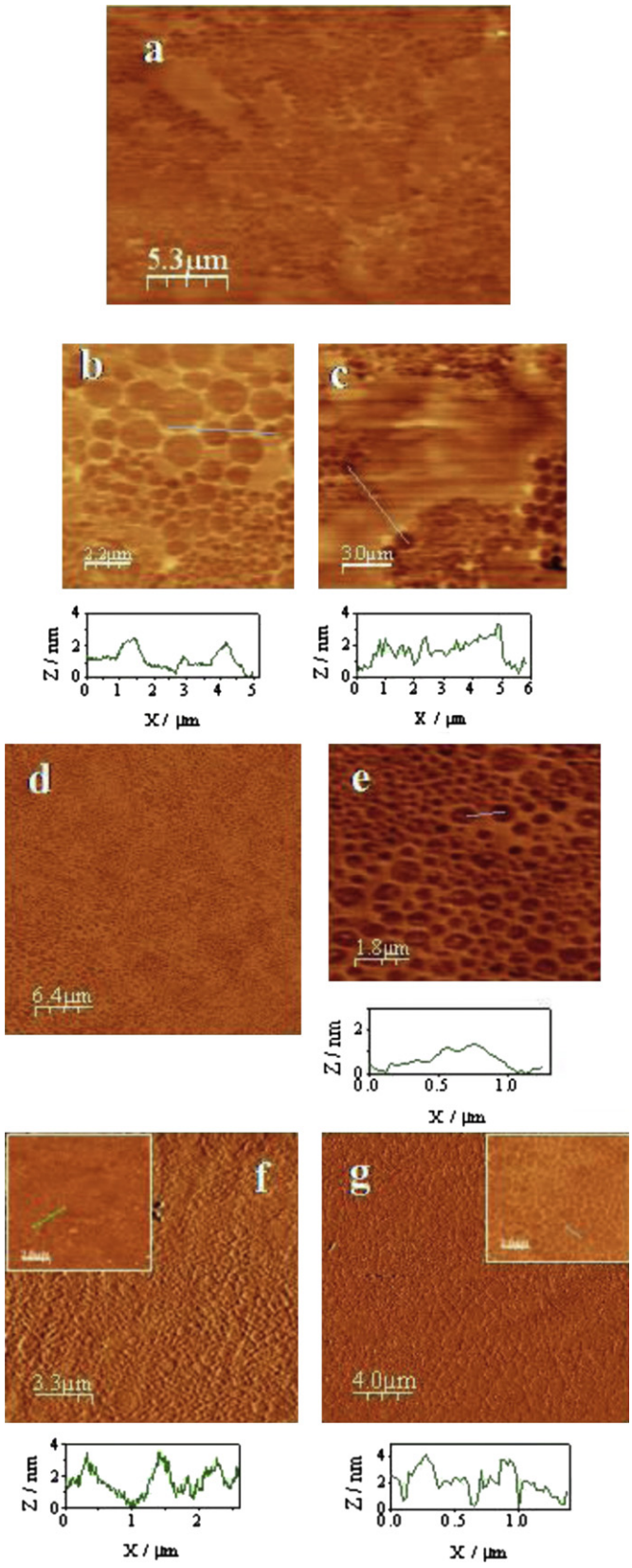

Fig. 6. AFM images of LB films of PMAO/Gemini/QDs mixed monolayers prepared by keeping X_{Matrix} constant at 0.98 and the following polymer composition in the mixed matrix: (a–c)$Y_{PMAO} = 0.1$; (d, e) $Y_{PMAO} = 0.5$; (f) $Y_{PMAO} = 0.67$ and (g) $Y_{PMAO} = 0.8$. The surface pressure of the Langmuir monolayers precursors of the LB films was 30 mN m^{-1}.

highest QDs coverage using matrices prepared exclusively with PMAO or Gemini surfactant.

Fig. 5a presents the surface pressure–concentration isotherms for different mixed films and Fig. 5b shows the elasticity values against surface pressure plot of these films. The surface pressure/concentration isotherms of monolayers with mixed matrices are located between those prepared with matrices of one component, PMAO or the surfactant, when the matrix composition, Y_{PMAO}, is below 0.33. Above this value the isotherms are shifted to higher surface concentrations than that corresponding to the polymer PMAO/QDs. On the other hand, the elasticity isotherms in Fig. 5b, show a weak synergistic effect when the polymer mole fraction in the matrix is above 0.33, reaching the highest values for mixed monolayers with polymer mole fraction around 0.5 (Y_{PMAO} from 0.5 to 0.67). From the results, it is possible to conclude that the organization of molecules at the monolayer evolves with the matrix composition and renders the most condensed and elastic states when the matrix composition, Y_{PMAO}, is around 0.5. Attractive interactions between the polymer and the surfactant molecules can be responsible for this efficient packing.

We transferred Langmuir monolayers of these films from the air–water interface onto the solid substrate. The evolution of the domains' morphology with the concentration of PMAO in the mixed matrices can be observed in Fig. 6. The AFM image in Fig. 6a corresponds to the LB film with $Y_{PMAO} = 0.1$, and it shows the presence of different kinds of domains, hexagonal network and agglomerates. Magnification of these domains is presented in Fig. 6b and c, respectively. As can be seen in Fig. 6b and c, the architecture of these domains is similar to those observed in monolayers of PMAO/QDs and surfactant/QDs, respectively. This fact means that the two different dewetting mechanisms detected in the PMAO/QDs and Gemini/QDs mixed films can be observed in the films containing mixed matrices with $Y_{PMAO} \leq 0.3$. As expected, when the polymer composition in the matrix increases, the dewetting process characteristic of the polymer matrix becomes more important and prevails over the dewetting mechanism corresponding to the surfactant matrix. This behavior is observed when the polymer concentration reaches the value of $Y_{PMAO} = 0.5$, as shown in Fig. 6d and e. To gain insight into the effect of the composition on the structure of the hexagonal network, we have carried out the statistical analysis of the dimensions of the holes and rims, as shown in Table 1. Comparison between the hole size of films prepared with mixed PMAO/surfactant matrices and with the PMAO matrix shows that the polymer PMAO provides the smallest holes. Moreover, the rim size of PMAO/QDs films is also the smallest one. On the other hand, the holes corresponding to the hexagonal networks for LB films prepared with mixed matrices and Y_{PMAO} values around 0.5 present the lowest polydispersity degree.

We determined the roughness of the rims from the AFM profiles. Results show that it is independent of the film composition and the average value of 3–4 nm, is compatible with the diameter of the QDs dissolved in chloroform (3.4 ± 0.1) nm. The thickness value obtained by ellipsometry, (4.8 ± 0.3) nm, was also compatible with this value.

4. Conclusions

We have analyzed the effect of the surface composition on the structure of QDs self-assemblies by modifying the Langmuir monolayers precursors of the LB films. We chose the polymer PMAO and the cationic Gemini surfactant 18-2-18 as matrices to assist in the self-assembly process. Our results demonstrated that the QDs agglomeration is avoided by the addition of both the polymer PMAO and the surfactant 18-2-18. Attractive interactions between the chains of these compounds and the hydrophobic

moiety of the QDs stabilizer, TOPO, lead to the adsorption of QDs on the matrices while the hydrophilic group of the polymer or surfactant improves the QDs adsorption on the solid substrate, avoiding the nanoparticle agglomeration.

Our results also show two different film features depending on the matrix composition. Thus, when the matrix is exclusively composed of the polymer PMAO, a continuous network of hexagonal domains with QDs adsorbed on the rims was observed. In contrast, when the monolayer is built with a mixture of surfactant and QDs, an array of droplets was produced. The differences were attributed to distinct dewetting processes, nucleation and growth of holes and spinodal dewetting, for PMAO/QDs and surfactant/QDs films, respectively.

Our results allow us to conclude that in films composed of PMAO/Gemini mixed matrices, the dewetting mechanism characteristic of the polymer, namely coalescence of holes, prevailed over the surfactant dewetting mechanism, spinodal mechanism, even in films with small amounts of polymer PMAO in the matrix. This is likely due to the high molecular weight of the polymer compared with the one of the surfactant molecule. Thus, taking into account that the molecular weight of the polymer is around 50 times higher than the surfactant one, and that the polymer dewetting mechanism is addressed by the gravitational effect, while the capillary waves address the spinodal one, it is expected that the gravitational effect prevailed over the capillary waves even in films with small amount of polymer.

Finally, our results show that is possible to modulate the self-assembly of QDs by modifying the surface composition of the Langmuir monolayer precursors of the LB films by the addition of the polymer PMAO or the Gemini surfactant 18-2-18. This strategy can be presented as a bottom-up reproducible methodology for patterning at nanoscale.

Acknowledgments

The authors thank financial support from ERDF and MEC (MAT 2010-19727). T. Alejo wishes to thank the European Social Fund and Consejería de Educación de la Junta de Castilla y León for her FPI grant. We are grateful to the UIRC of the Universidad Complutense de Madrid for making available the ellipsometry facility, in particular, JEF Rubio for the ellipsometric measurements. We also thank to Ultra-Intense Lasers Pulsed Center of Salamanca (CLPU) for the AFM measurements and to Dr B. Rodriguez and International Iberian Nanotechnology Laboratory (INL) for the FIB/SEM facility.

References

[1] K.M. Langner, G.J.A. Sevink, Soft Matter 8 (2012) 5102–5118.
[2] J. Huang, F. Kim, A.R. Tao, S. Connor, P. Yang, Nat. Mater. 4 (2005) 896–900.
[3] A.R. Tao, J. Huang, P. Yang, Acc. Chem. Res. 41 (2008) 1662–1673.
[4] N. Tomczak, D. Janczewski, M. Han, G.J. Vancso, Prog. Polym. Sci. 34 (2009) 393–430.
[5] a) R. Sknepnek, J.A. Anderson, M.H. Lamm, J. Schmalian, A. Travesset, ACS Nano 2 (2008) 1259–1265;
b) A.C. Balazs, Curr. Opin. Colloid Interface Sci. 4 (2000) 443–448;
c) J.Y. Lee, Z. Shou, A. Balazs, Macromolecules 36 (2003) 7730–7739.
[6] B.H. Shon, S.I. Yoo, B.W. Seo, S.H. Yun, S.M. Park, J. Am. Chem. Soc. 123 (2001) 12734–12735.
[7] B.H. Shon, J.M. Choi, S.I. Yoo, S.H. Yun, W.C. Zin, J.C. Jung, M. Kanehara, T. Hirata, T. Teranishi, J. Am. Chem. Soc. 125 (2003) 6368–6369.
[8] Y. Lin, A. Böker, J. He, K. Sill, H. Xiang, C. Abetz, X. Li, J. Wang, T. Emrick, S. Long, Q. Wang, A. Balazs, T.P. Russell, Nature 434 (2005) 55–59.
[9] H. Li, R. Sachsenhofer, W.H. Binder, T. Henze, T. Thurn-Albrecht, K. Busse, J. Kressler, Langmuir 25 (2009) 8320–8329.
[10] R.B. Cheyne, M.G. Moffitt, Langmuir 21 (2005) 10297–10300.
[11] C.B. Murray, C.R. Kagan, M.G. Bawendi, Annu. Rev. Mater. Sci. 30 (2000) 545–610.
[12] J.M. Krans, J.M. van Rutenbeek, V.V. Fisun, I.K. Yanson, L.J. de Jongh, Nature 375 (1995) 767–769.
[13] J. Jin, L.S. Li, Y.Q. Tian, Y.J. Zhang, Y. Liu, Y.Y. Zhao, T.S. Shi, T.J. Li, Thin Solid Films 327–329 (1998) 559–562.
[14] Y.S. Kang, S. Risbud, J. Rabolt, P. Stroeve, Langmuir 12 (1996) 4345–4349.
[15] A. Gole, N.R. Jana, S.T. Selvan, J.Y. Ying, Langmuir 24 (2008) 8181–8186.
[16] K.M. Gattás-Asfura, C.A. Constantine, M.J. Lynn, D.A. Thimann, X. Ji, R.M. Leblanc, J. Am. Chem. Soc. 127 (2005) 14641–14646.
[17] Y.-J. Shen, Y.-L. Lee, Y.-M. Yang, J. Phys. Chem. B 110 (2006) 9556–9564.
[18] Y. Tian, J.H. Fendler, Chem. Mater. 8 (1996) 969–974.
[19] H. Li, X. Wang, Sensors and Actuators B 134 (2008) 238–244.
[20] H. Li, X. Wang, Z. Gao, Z. He, Nanotechnology 18 (2007) 205603–205608.
[21] F.M. Menger, C.A. Littau, J. Am. Chem. Soc. 115 (1993) 10083–10090.
[22] M.X. Liu, L.H. Gan, G. Chen, Z.J. Xu, Z.X. Hao, L.W. Chen, Chin. Chem. Lett. 17 (2006) 1085–1088.
[23] M.X. Liu, L.H. Gan, Z.X. Hao, G. Chen, L.W. Chen, Colloid Surf. A Physicochem. Eng. Asp. 301 (2007) 432–436.
[24] M.X. Liu, L.H. Gan, Y. Zeng, Z. Xu, Z.X. Hao, L.W. Chen, J. Phys. Chem. C 112 (2008) 6689–6694.
[25] A. Guerrero-Martínez, J. Pérez-Juste, E. Carbó-Argibay, G. Tardajos, L. Liz-Marzán, Angew. Chem. Int. Ed. 48 (2009) 9484–9488.
[26] T. Alejo, M.D. Merchán, M.M. Velázquez, Thin Solid Films 519 (2011) 5689–5695.
[27] K. Holmberg, B. Jönsson, B. Kronberg, B. Lindman, Surfactants and Polymers in Aqueous Solution, second ed., John Wiley and Sons, LTD, Chichester, 2003.
[28] C. Delgado, M.D. Merchán, M.M. Velázquez, J. Phys. Chem. B 112 (2008) 687–693.
[29] M.D. Merchán, M.M. Velázquez, Colloid Surf. A Physicochem. Eng. Asp. 366 (2010) 12–17.
[30] R. Ribera, M.M. Velázquez, Langmuir 15 (1999) 6686–6691.
[31] D. López-Díaz, M.M. Velázquez, Eur. Phys. J. E 26 (2008) 417–425.
[32] S. Gupta, N. Singh, M. Sastry, R. Kakkar, R. Pasricha, Thin Solid Films 519 (2010) 1072–1077.
[33] S.E. Heisig, M.D. Merchán, M.M. Velázquez, J. Colloid Sci. Biotechnol. 1 (2012) 33–41.
[34] R. Zana, M. Benrraou, R. Rueff, Langmuir 7 (1991) 1072–1075.
[35] W.W. Yu, X. Peng, Angew. Chem. Int. Ed. Engl. 41 (2002) 2368–2371.
[36] W.W. Yu, L. Qu, W. Guo, X. Peng, Chem. Mater. 15 (2003) 2854–2860.
[37] H.G. Tompkins, A User's Guide to Ellipsometry, Academic Press Inc, London, 1993.
[38] B. Martín-García, M.M. Velázquez, J.A. Pérez-Hernández, J. Hernández-Toro, Langmuir 26 (2010) 14556–14562.
[39] E.D. Palik, Handbook of Optical Constant of Solid, Academic Press Inc., San Diego, 1993.
[40] A.M. Gonçalves da Silva, M.I. Viseu, C.S. Campos, T. Rechina, Thin Solid Films 320 (1998) 236–240.
[41] B. Martín-García, M.M. Velázquez, Mater. Chem. Phys., submitted for publication.
[42] J.T. Davies, E.K. Rideal, Interfacial Phenomena, Academic Press, New York, 1963, p. 265.
[43] D. Gentili, G. Foschi, F. Valle, M. Cavallini, F. Biscarini, Chem. Soc. Rev. 41 (2012) 4430–4443.
[44] A. Sharma, E. Ruckenstein, J. Colloid Interface Sci. 137 (1990) 433–445.
[45] A. Sharma, J. Colloid Interface Sci. 156 (1993) 96–103.
[46] G. Debregas, F. Brochard-Wyart, J. Colloid Interface Sci. 190 (1997) 134–141.
[47] S.W. Sides, B.J. Kim, E.J. Kramer, G.H. Fredrickson, Phys. Rev. Lett. 96 (2006) 250601.
[48] F.D.A.A. Reis, Macromolecules 41 (2008) 8932–8937.
[49] G. Reiter, Phys. Rev. Lett. 68 (1992) 75–78.
[50] R. Li, Q. Chem, D. Zhang, H. Lui, Y. Hu, J. Colloid Interface Sci. 327 (2008) 162–168.